

# Growth and Characterization of Pure and L Histidine doped Glycine Sodium Nitrate Single Crystal

<sup>[1]</sup> S.R. Balaji, <sup>[2]</sup> T. Balu, <sup>[3]</sup> T.R. Rajasekaran

<sup>[1]</sup> Post Graduate Department of Physics, V.O.Chidambaram College, Tuticorin 628 008, India

<sup>[2]</sup> Department of Physics, Aditanar College of Arts and Science, Tiruchendur 628 216, India

<sup>[3]</sup> Department of Physics, Manonmaniam Sundaranar University, Abishekapatty, Tirunelveli 627 012, India

**Abstract-** Single crystals of GSN and different molar concentration of L-Histidine doped GSN crystals; have been grown from aqueous solution by slow evaporation method. Solubility studies of grown crystals for different temperatures prove the positive temperature coefficient of solubility. The crystals were subjected to Powder X-ray diffraction, which identifies that all the grown crystals where belong to monoclinic system. Fourier transform infra-red spectra shows that the doped and pure GSN provides similar spectra, but there is shift observed for all the peaks suggesting that there is wide range of interactions for the grouping. UV-Vis-NIR absorption spectra helps us to identify that the lower cut-off wavelength is  $217 \pm 1$  nm for pure and L- Histidine doped GSN single crystals. Vickers microhardness measurements reveal that the hardness values of the crystal decreases due to the increase in the dopant ratio except at 4 mole% doping. Photoluminescence spectrum (PL) result shows that the crystals shows a strong and broad emission peak at around 528nm which illustrate that the crystals has an emission of green radiations.

**Keywords:** - Single crystals; Doping; Solubility; PXRD; FTIR; UV-Vis-NIR; Photoluminescence.

## I. INTRODUCTION

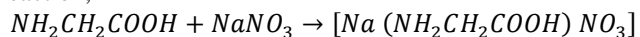
Nanotechnology can be understood as a technology of design, fabrication and applications of nanostructures and nanomaterials, as well as fundamental understanding of physical properties and phenomena of nanomaterials and nanostructures [1]. Metal oxides nanostructures play crucial role in many areas of chemistry, physics and materials science [2]. The different properties of oxides enable the numerous applications in the fabrication of microelectronic circuits, sensors, piezoelectric devices, fuel cells, coatings against corrosion and as catalysts (most catalysts involve an oxide as active phase). ZnO is an important metal oxides that could be easily grown, environmental friendly and of interest to many applications. It is suitable for industrial, technical and medical applications due to its diverse properties which have been found to strongly depend on their morphology [3] and thus has been the subject of study by many researchers. Various methods have been reported for the synthesis of ZnO nanoparticles, including precipitation, hydrothermal, sol-gel, thermal evaporation and mechanochemical methods. The mechanochemical method is one of the most frequently utilized methods for the synthesis of ZnO nanoparticles due to its excellent advantages such as low cost, low temperature, non-toxic operation and environmental friendliness. Since such reactions do not involve organic solvents, therefore for controlling the nucleation and growth of nanoparticles, they are attractive from an environmental point of view.

Zinc oxide nanoparticles have been extensively used as anticorrosive coatings on metals. A number of methods for the protection of metals against corrosion are recently focused on the possible use of metal oxide nanoparticles as either film forming corrosion inhibitors or in protective coatings [4]. This study describes the process of synthesizing and characterization of ZnO nanoparticles and then evaluating their anticorrosion performance using electrochemical studies were carried out in 0.1M HCl on mild steel.

## II. EXPERIMENTAL

### A. Synthesis

Glycine Sodium Nitrate (GSN) growth solution was prepared by dissolved analar grade glycine (Merck) and sodium nitrate (Merck) in stoichiometric ratio 1:1 in double distilled water to yield a homogeneous mixture of solution. The polycrystalline starting material was synthesized by evaporating the solution to almost dryness according to the reaction,



The purity of the synthesized salt was improved by successive recrystallization process. Four different concentration (2, 4, 6 and 8mole %) of L-Histidine were taken as a dopant material for GSN crystal.

### B. Crystal growth

GSN and L-Histidine doped single crystals were grown by slow evaporation technique. Recrystallized salt of pure and

L-Histidine doped GSN was taken as raw material. Saturated solutions were prepared at room temperature with water as solvent. The prepared solution was taken in petri dishes after filtration and closed with perforated covers and kept in dust free atmosphere. The grown crystals are shown in figure 1-5.

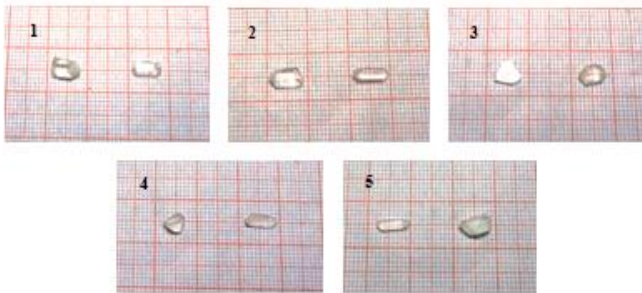


Fig. 1-5. Pure, 2,4,6 and 8 mole % doped GSN crystals

**C. Solubility**

The solubility of GSN doped with L-Histidine of different molar concentration in water was determined as a function of temperature in the temperature range 35 – 50o C. The experimentally observed solubility curve is shown in the figure 6. The diagram shows that, the solubility increases linearly with increase of temperature and the increase in percentage of dopant.

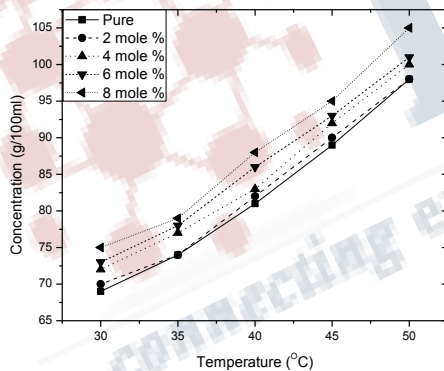


Fig 6: Solubility curve of GSN doped with L-Histidine of different molar concentration in aqueous solution

**III. RESULT AND DISCUSSION**

**A. Powder X-Ray Diffraction**

The samples of the grown crystals have been crushed to a uniform fine powder and subjected to powder X-ray diffraction using a Panalytical X’Pert Powder X’Celerator Diffractometer. From the powder X-ray diffraction data, the lattice parameters and the cell volume have been calculated and are given in table 1.

Table 1: Lattice parameter values of pure and L-Histidine doped GSN crystals.

Parameters	Pure	2 mole %	4 mole %	6 mole %	8 mole %
a	14.338	14.325	14.319	14.312	14.313
b	5.2279	5.2362	5.2361	5.2363	5.2368
c	9.1704	9.1698	9.1696	9.1695	9.1692
$\alpha, \gamma$	90°	90°	90°	90°	90°
$\beta$	119.0462°	119.0623°	119.0599°	119.0568°	119.0561°
V (Å <sup>3</sup> )	600.8515	601.2365	601.2442	601.2498	601.2503
System	Monoclinic	Monoclinic	Monoclinic	Monoclinic	Monoclinic

**B. FTIR analysis**

Infra-red spectroscopic studies were carried out on the grown crystals in order to understand the structure and bonding in them. Fourier Transform Infrared (FTIR) spectrum was recorded using KBr pellet technique on a Thermo Nicolet, Avatar 370 spectrophotometer. The FTIR spectrum was recorded in the range 400 - 4000 [(cm)<sup>-1</sup>] to identify the functional group present in GSN and L-Histidine doped GSN crystals. The spectrum shows a broad band between 2400 and 3400 [(cm)<sup>-1</sup>] resulting from superimposed O-H and [(NH)<sub>3</sub><sup>+</sup>] stretching band. Although L-Histidine doped GSN spectrum provides similar features as that of pure GSN spectrum, there is a shift observed for all the peaks suggesting that there is wide range of interaction for the grouping. The results are presented in table 2.

Table 4.2: Assignments of IR band frequencies of pure and L-Histidine doped GSN

(Wavenumbers in cm <sup>-1</sup> )					Assignments
Pure	2 mole %	4 mole %	6 mole %	8 mole %	
3248.77	3248.70	3248.29	3248.48	3248.37	$\nu_3$ (C-H)
2891.77	2890.12	2887.79	2887.53	2891.28	$\nu_1$ (O-H)
2275.18	2275.09	2275.27	2275.13	2275.05	$\delta_{as}$ (C-C)
2011.89	2011.48	2011.86	2011.90	2012.38	$\nu_1$ (N-H)
1756.45	1769.13	1769.45	1769.20	1769.45	$\nu_1$ (C-H)
1617.64	1618.52	1617.68	1618.72	1617.79	$\nu$ (C-C)
1381.92	1379.81	1382.77	1382.35	1381.27	<i>op</i> (C-O-H)
1117.18	1117.34	1117.28	1117.26	1117.30	$\nu$ (C-H)
937.28	937.28	937.36	937.27	937.62	$\delta$ (N-O)
891.22	891.13	891.34	891.21	891.61	$\omega$ (C-O)
829.91	829.98	830.13	830.10	830	<i>op</i> (C-H)
676.81	676.95	677.01	677.01	677.11	$\delta$ (C-H)
586.25	586.64	586.53	586.40	586.58	$\delta$ (C-O)

**C. UV-Vis-NIR spectral study**

To determine the transmission range and hence to know the suitability of pure and L-Histidine doped GSN single crystals for optical applications, the UV-Vis-NIR spectrum was recorded in the range of 190–1100 nm, which covers near ultraviolet, visible and then near-infrared regions, using

Perkin Elmer Lambda 35 UV spectrophotometer. The UV-Vis-NIR absorbance spectra of pure and L-Histidine doped GSN are shown in fig.7. It is found that the lower cut-off wavelength are 216nm, 218nm, 217nm, 218nm and 218nm for pure GSN, GSN + 2 mole%, GSN + 4 mole%, GSN + 6 mole% and GSN + 8 mole% respectively.

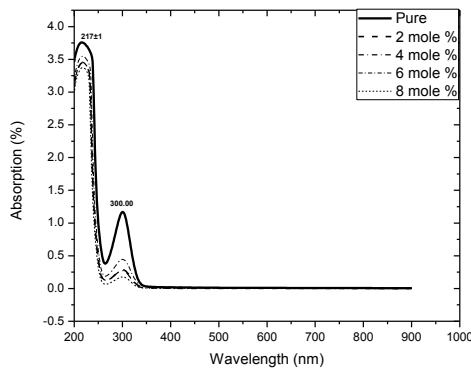


**Fig 7. UV – Vis – NIR spectrum of pure and doped GSN**  
The result shows that the crystal has sufficient transmission in the entire visible and IR region. From the figure it is also observed that the absorption coefficient of L-Histidine doped GSN is less than that of pure GSN. Among the L-Histidine doped GSN the absorption coefficient for 8 mole% L-Histidine doped GSN is found to be least than that of the pure GSN and other concentrations. The wide transmission shown in the entire visible region (200-900nm) of our grown crystals, confirms that these materials may be a potential candidate for opto-electronic applications.

**D. Microhardness studies**

Microhardness testing is one of the best methods of understanding the mechanical properties of materials such as fracture behavior, yield strength, brittleness index and temperature of cracking. Hardness measurements were carried out on GSN and L-Histidine doped GSN crystals using Shimadzu HMV – 2 microhardness tester fitted with Vickers diamond pyramidal indenter. The well-polished crystal was mounted on the platform of the microhardness tester and the loads of different magnitudes were applied over a fixed interval of time. Vickers microhardness number was evaluated from the relation

$$H_v = 1.8544 (P/d^2) \text{ kg/mm}^2$$

where  $H_v$  is the Vickers hardness number,  $P$  is the indenter load in kg and  $d$  is the diagonal length of the impression in mm. Figure 8, shows that the hardness number increases with the increase of the applied load. This behavior of increasing microhardness with the load is known as reverse indentation size effect (RISE) [8]. From the microhardness studies we came to know that the hardness values of the crystal decreases due to the increase in the dopant ratio

except in 6 mole % where we can observe the increase in the hardness value.

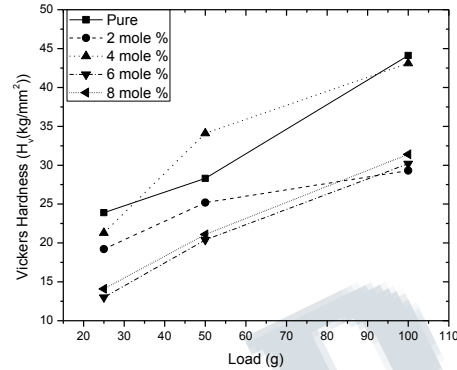


**Fig 8. Vickers hardness versus load for pure and different molar concentration L-Histidine doped GSN**

**E. Photoluminescence Studies**

Photoluminescence is the phenomenon in which electronic states of solids are excited by light of particular energy and the excitation energy is released as light. The photon energies reflect the variety of energy states that are present in these materials. Photoluminescence spectrum was recorded between 375 and 800 nm using the instrument F-7000 FL Spectrophotometer. The recorded PL spectrum of GSN and GSN doped with L-Histidine of different molar ratio crystals are shown in Fig.9-13. From the PL spectrum, a strong and broad emission peak was identified at around 528nm and illustrate that the GSN has an emission of green radiations.

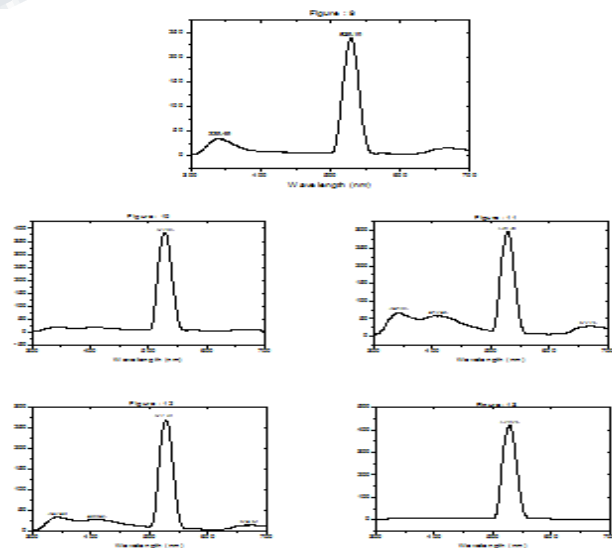


**Fig. 9-13. PL spectra of Pure, 2,4,6 and 8 mole % doped GSN crystals respectively**

#### IV. CONCLUSIONS

Single crystals of GSN and different molar concentration of L-Histidine doped GSN crystals; have been grown from aqueous solution. Solubility of GSN and L-Histidine doped GSN for different temperatures was estimated, which shows the crystals have positive temperature coefficient of solubility. Grown crystals of pure and L-Histidine doped GSN crystals were subjected to Powder X-ray diffraction to identify the crystallinity and also to identify the lattice parameters, the study shows that all the crystals crystallizes monoclinic system. Though the additives concentration is varied with different molar concentration, it does not alter the parent crystal system.

Fourier transform infra-red spectra of the grown crystals were recorded in the wave number range 400-4000 cm<sup>-1</sup>. Although L-Histidine doped GSN spectra provides similar features as that of pure GSN spectrum, there is shift observed for all the peaks suggesting that there is wide range of interactions for the grouping.

UV-Vis-NIR Spectrophotometer was employed to record absorbance spectra in the wavelength range 200 -900 nm. It is found that the lower cut-off wavelength are 216nm, 218nm, 217nm, 218nm and 218nm for pure GSN, GSN + 2 mole%, GSN + 4 mole%, GSN + 6 mole% and GSN + 8 mole% respectively. It also shows that, there is no any wide difference in the cutoff frequency due to inclusion of dopants, but the deep observations shows that there is a drop in the percentage of absorption due the dopants. The wide transmission shown in the entire visible region (200-900nm) of our grown crystals, confirms that these materials may be a potential candidate for opto-electronic applications.

The hardness study reveals that the hardness values of the crystal decreases due to the increase in the dopant ratio except in 6 mole %. Photoluminescence spectrum (PL) was recorded between 375 and 800 nm, the result shows that pure GSN and L-Histidine doped GSN shows a strong and broad emission peak at around 528nm which illustrate that the GSN has an emission of green radiations.

#### V. ACKNOWLEDGMENT

First author is thankful to the UGC for providing financial assistance through minor research project (File No: F MRP-5869/15 (SERO/UGC) – January 2015).

The authors sincerely thank Mr. Y. Vincent Sagayaraj, Archbishop Casmir Instrumentation Center (Tiruchirappalli) for recording FTIR, UV spectrum, Microhardness and Photoluminescence studies.

#### References

- [1] C. Ramachandra Raja, B. Vijayabhaskaran, Indian J. Pure & Appl. Phys. 49 (2011) 531.
- [2] R. Pepinsky, Y. Okaya, D.P. Eastman, T. Mitusui, Phys. Rev. 107 (1957) 1538.
- [3] R. Pepinsky, K. Vedam, Y. Okaya, Phys. Rev. 110 (1958) 1309.
- [4] A. Deepthy, H. L. Bhat, J. Cryst. Growth. 226 (2001) 287.
- [5] S. Dinakaran, Verma Sunil, S. Das Jerome, G. Bhagavannarayana, S. Kar, K.S. Bartwal, Appl. Phys. B: Lasers and Optics. 103 (2011) 2375.
- [6] S. Dinakaran, Verma Sunil, S. Das Jerome, Cryst. Eng. Comm. 13 (2011) 2375.
- [7] C. Chen, N. Ye, J. Lin, J. Jiang, W. Zing, B. Wu B, Adv. Matter. 113 (1999) 107.
- [8] K. Sangwal, Mat. Chem. and Phys. 63, 145 (2000).